SUPPORTING INFORMATION

Spatial variations of methane emission in a large and shallow eutrophic lake in subtropical climate

Qitao Xiao[1], Mi Zhang[1, *], Zhenghua Hu[1], Yunqiu Gao[1], Cheng Hu[1], Cheng Liu[1], Shoudong Liu[1], Zhen Zhang[1], Jiayu Zhao[1], Wei Xiao[1], X Lee[1,2, *]

Contents:

Figure S1. Effects of storage time on the dissolved methane concentration using water samples collected at BFG (a) and MLW (b). Each treatment was replicated three times. Error bars are one standard deviation. CTRL: measurement was made without delay. NS: difference from CNTRL is not statistically significant.

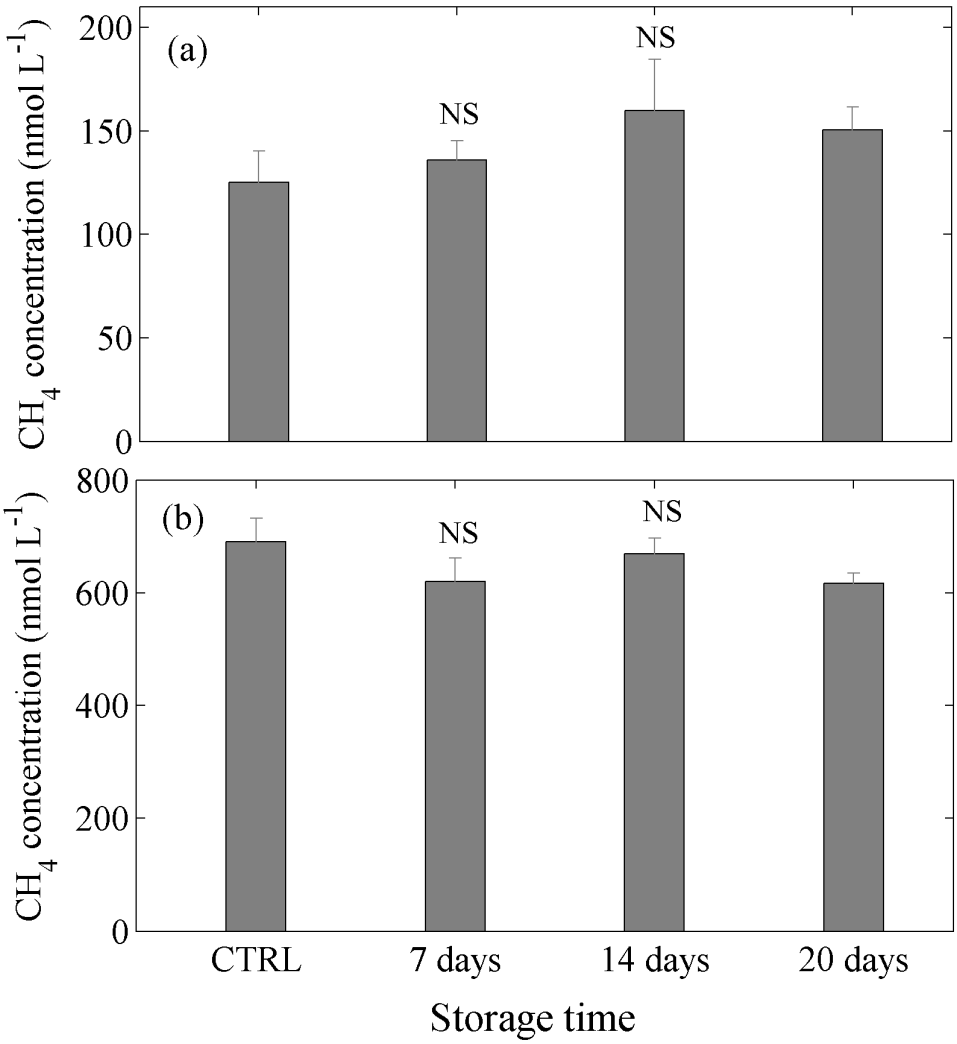

Figure S2. Effects of headspace fraction on the dissolved methane concentration using water samples collected at a local pond (a) and at MLW (b). Each treatment was replicated three times. Error bars are one standard deviation.

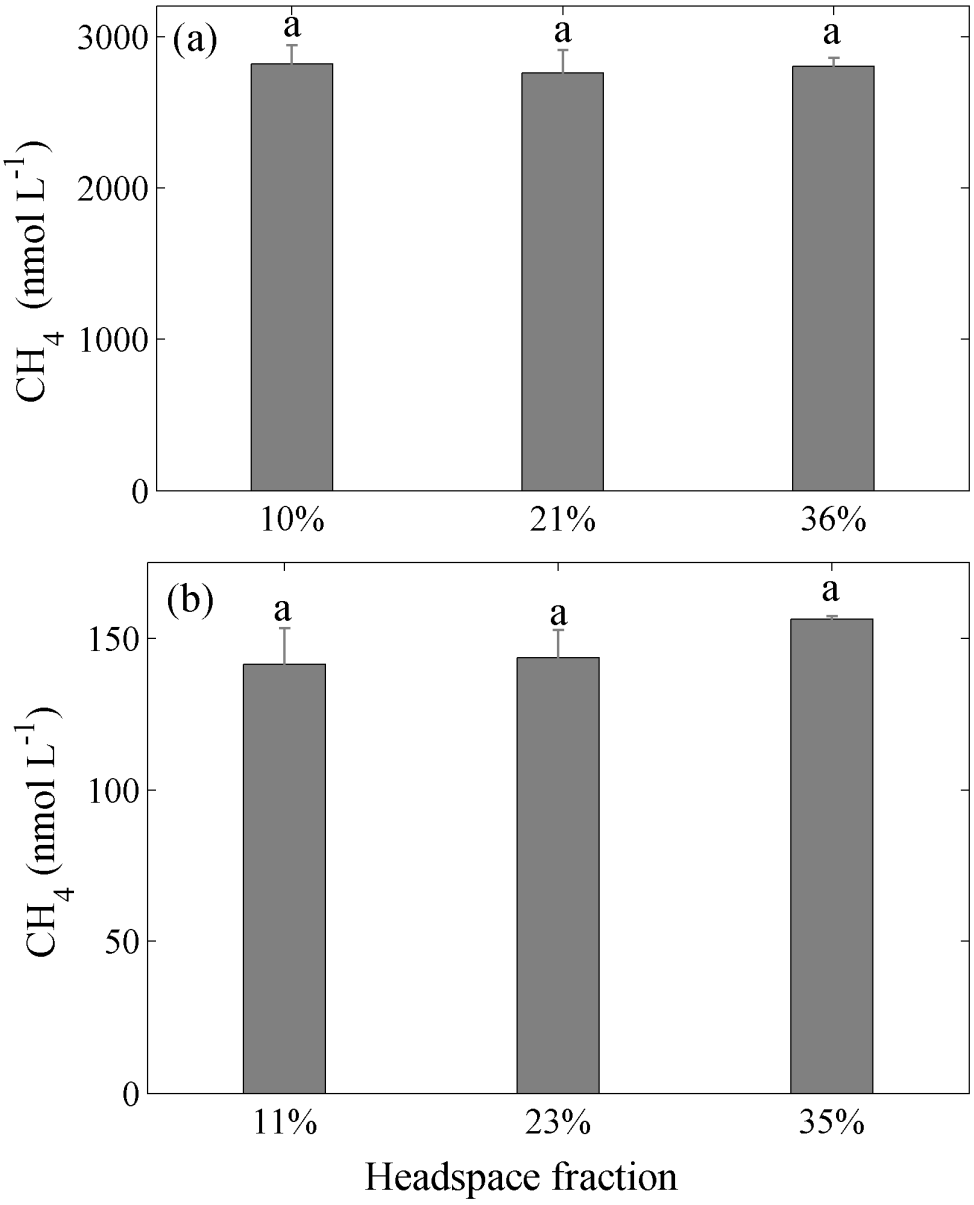

Figure S3. A diel composite of pH observed at the 20-cm depth at a buoy site in Gonghu Bay (location labeled as SSC in the map inset). Observations were made over 155 days in the summer of 2009 and in the winter of 2009-2010 (Hu *et al*., 2015).

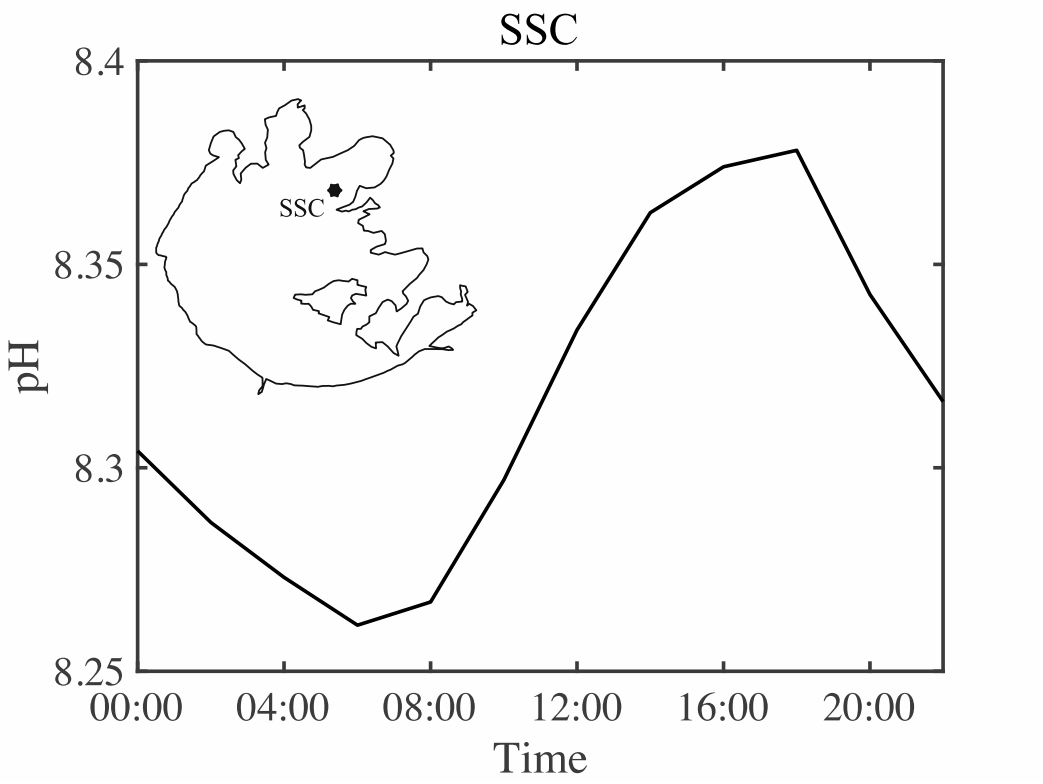

Figure S4. Temporal variation of the surface dissolved CH_4 at the five lake observation sites (MLW, BFG, DPK, XLS, and PTS) where frequent water sampling took place. Their locations are shown in Figure 1. Red circles indicate the whole-lake mean dissolved CH_4 concentration. The error bar is ±1 standard deviation.

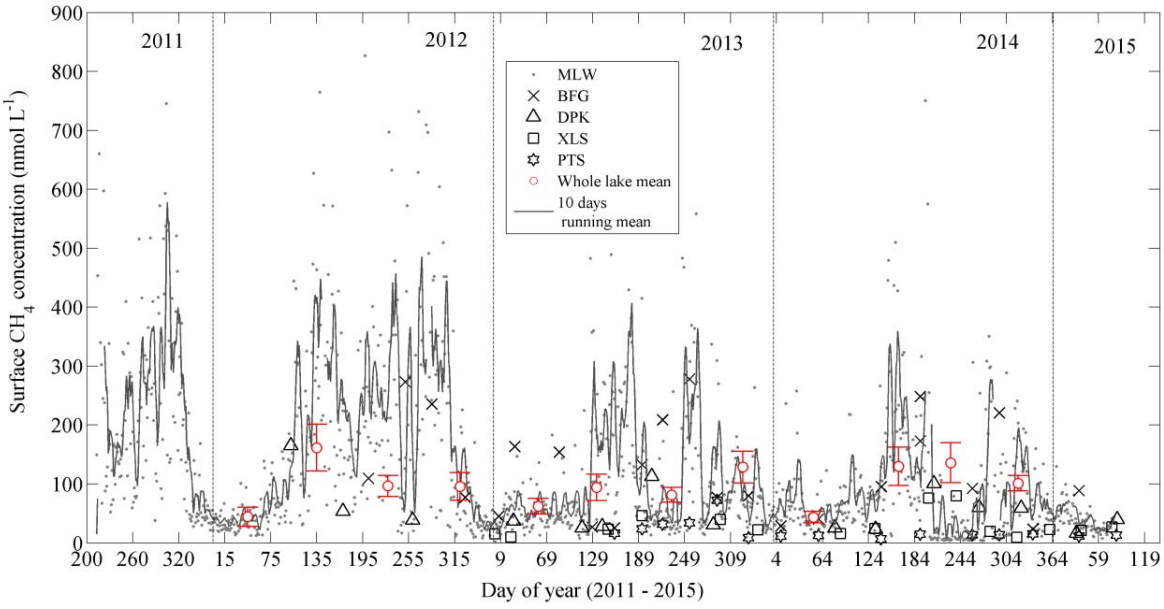

Figure S5. Temporal variation of wind speed at the five lake observation sites (MLW, BFG, DPK, XLS, and PTS) where frequent water sampling took place. Their locations are shown in Figure 1.

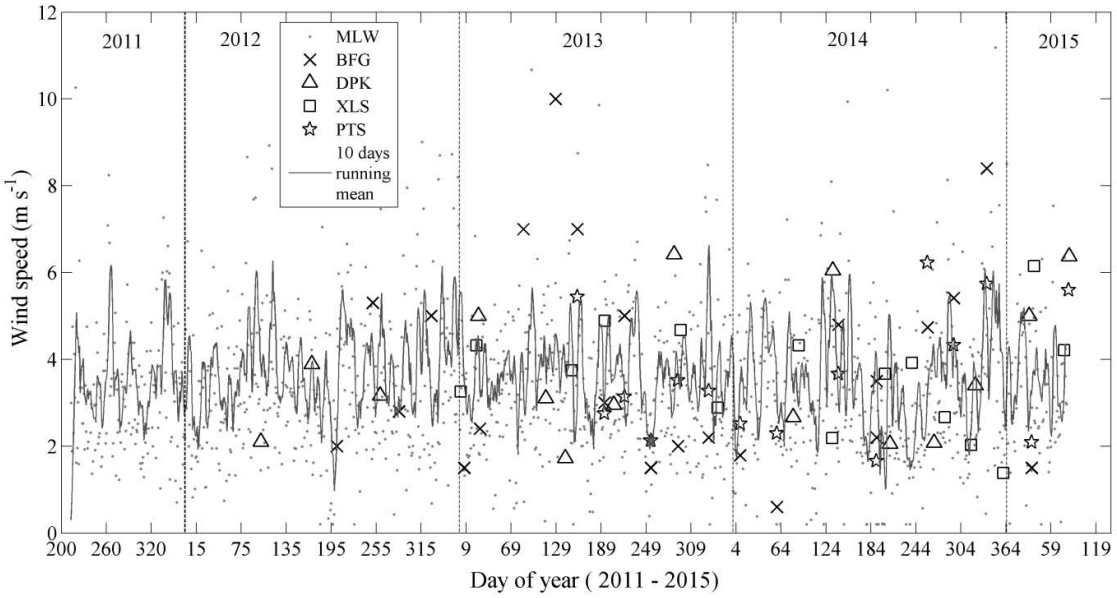

Figure S6. Diel variation of the diffusion CH_4 flux at MLW. The gas transfer coefficient was determined with the model described by Cole *et al.* (1998, a), and with a model that considers both wind speed and waterside convection (Podgrajsek *et al.,* 2015, b). Error bars are ± 1 standard error.

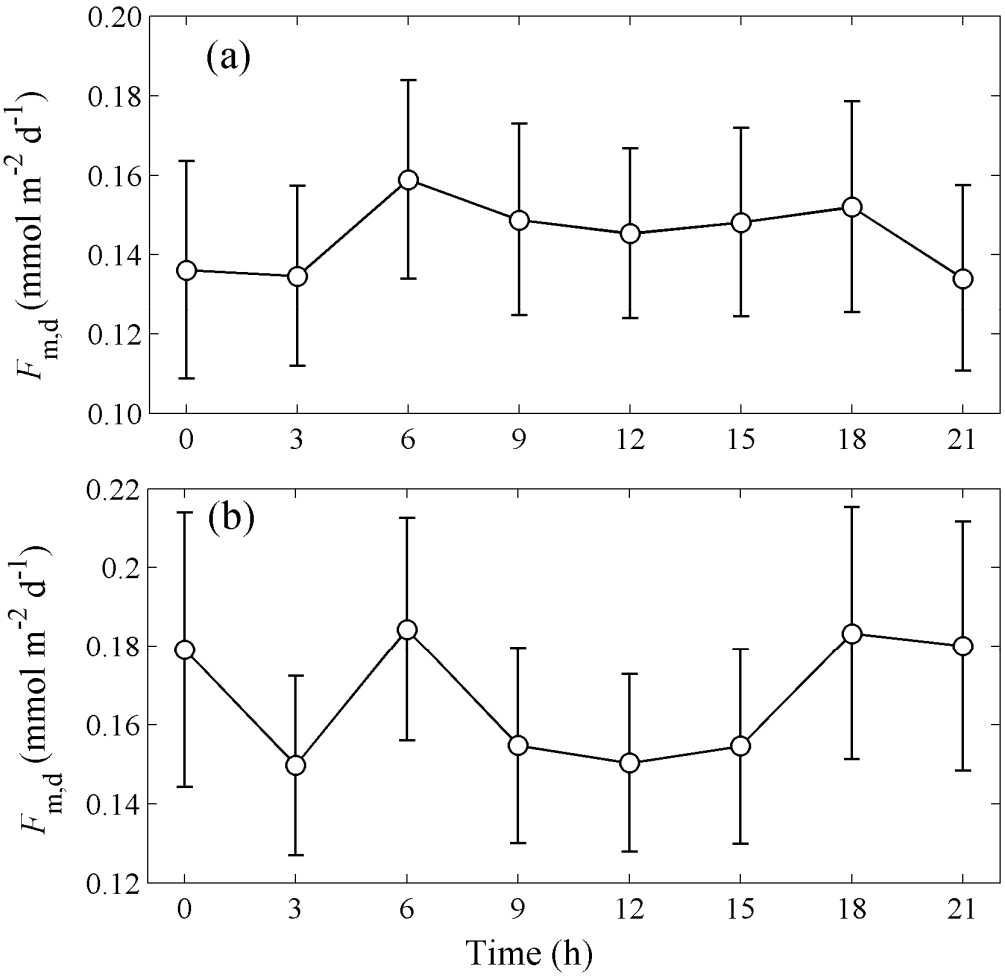

Table S1. Annual mean total phosphorous (TP) and total nitrogen (TN) of the seven zones in Lake Taihu in 2014.

Zones	Area (km^2)	TP (mg L^{-1})	TN (mg L^{-1})	Trophic class[1]
Meiliang Bay	100	0.087	2.18	Eutrophic
Gonghu Bay	215.6	0.065	1.81	Mesotrophic
East Zone	316.4	0.033	1.23	Mesotrophic
Dongtaihu Bay	131	0.037	0.90	Mesotrophic
Southwest Zone	443.2	0.067	2.01	Mesotrophic
Northwest Zone	394.1	0.094	2.58	Hyper-eutrophic
Central Zone	737.5	0.072	1.89	Mesotrophic
Whole lake	2338	0.069	1.90	Eutrophic

Data source: The Health Status Report of Taihu Lake, Taihu Basin Authority of Ministry of Water Resources and Electric Power, http://www.tba.gov.cn/.

1: Trophic classifications are defined according to OECD (Organization for Economic Cooperation and Development) (1982), Eutrophication of Waters. Monitoring assessment and control. Final Report. OECD Cooperative Programme on Monitoring of Inland Waters (Eutrophication Control), Environment Directorate, OECD, Paris.

Table S2. Temporal correlation of the diffusion CH_4 flux (mmol m^{-2} d^{-1}) with wind speed (m s^{-1}) and dissolved CH_4 concentration (nmol L^{-1}) at five locations (MLW, BFG, DPK, XLS, and PTS**).**

Site	CH_4 concentration	Wind speed
MLW	y = 0.0011x – 0.0193 R = 0.92 p < 0.001 n = 1261	y = 0.0934x – 0.1852 R = 0.09 p < 0.001 n = 1264
BFG	y = 0.0015x – 0.0468 R = 0.84 p < 0.001 n = 24	y = 0.0514x – 0.0601 R = 0.21 p = 0.315 n = 24
DPK	y = 0.0010x – 0.0032 R = 0.93 p < 0.001 n = 15	y = -0.0255x +0.1470 R = -0.21 p = 0.458 n = 15
XLS	y = 0.0016x – 0.0164 R = 0.97 p < 0.001 n = 15	y = 0.0276x – 0.0688 R = 0.33 p = 0.223 n = 15
PTS	y = 0.0010x – 0.0028 R = 0.94 p < 0.001 n = 15	y = 0.0114x – 0.0232 R = 0.13 p = 0.654 n = 15

Table S3. Pearson correlation between these explanatory environmental variables measured at the 29 spatial sampling sites. DO, dissolved oxygen concentration; Chl-a, chlorophyll a concentration; Spc, specific conduce; ORP, oxidation reduction potential; NTU, turbidity; Depth, water depth; Clarity, water clarity.

	NDVI	DO	pH	Chl-a	NTU	Depth	Spc	ORP
NDVI								
DO	-0.02							
pH	-0.34*	0.72**						
Chl-a	0.31	0.70**	0.48**					
NTU	-0.61**	0.07	0.27	0.23				
Depth	0.01	0.25	0.43*	0.04	0.11			
Spc	0.291	-0.49**	-0.57**	0.43*	-0.35*	0.09		
ORP	-0.01	-0.18	-0.08	0.05	-0.20	-0.04	0.08	
Clarity	0.58**	0.12	-0.11	0.54**	-0.61	-0.23	-0.10	0.01

*, ** Correlation is significant at the 0.05, and 0.01 level, respectively.

Table S4. Summary of the general multiple regressions: variance inflation factor (VIF), R^2, significance levels of the predictor variables (*p*), and the Akaike information criterion (AIC).

Model	Explanatory variables	VIF	R^2	*p*	AIC
1	NDVI		0.27	0.004	-148.29
2	NDVI	1.51	0.40	0.001	-151.98
	Water clarity	1.51			
3	NDVI	1.52	0.63	<0.001	-164.19
	Water clarity	1.55			
	Dissolved oxygen	1.03			
4	NDVI	1.60	0.78	<0.001	-176.46
	Water clarity	1.75			
	Dissolved oxygen	1.14			
	Water depth	1.21			

Comparison of the diffusion flux calculated with four different models for the gas transfer coefficient

In this supplementary section, we present a comparison of the diffusion flux calculated using four different models for the gas transfer coefficient. The four models are described by Cole *et al*. (1998, k_1), Read *et al*. (2012, k_2), Heiskanen *et al*. (2014, k_3), and Podgrajsek *et al*. (2015, k_4).

The first model is that of Cole *et al*. (1998). In this model, the gas transfer coefficient k_1 is wind-dependent and is normalized to a Schmidt number 600 of a gas at temperature of 20 ^{o}C,

$$k_1 = k_{600} \times (S_c/600)^{-n} \quad \text{(S1)}$$

where S_c is Schmidt number for CH_4 at in-situ temperature. For the exponent n, we used the value 2/3 at low wind speed ($U_{10} < 3.7$ m s^{-1}) according to Huotari *et al*. (2009) and the value of 1/2 at high wind speed ($U_{10} > 3.7$ m s^{-1}) according to MacIntyre *et al*. (1995) and Juutinen *et al*. (2009). An empirical relationship was used to determine k_{600} (cm h^{-1}; Cole and Caraco, 1998):

$$k_{600} = 2.07 + 0.215U_{10}^{1.7} \quad \text{(S2)}$$

where U_{10} is wind speed at the 10-m height (m s^{-1}). The required input is U_{10}, which was measured by a wind sensor at PTS in the lake.

The second model is a surface renewal scheme described Read *et al*. (2012). It considers both wind shear (ε_u) and waterside convection (ε_w),

$$k_2 = \eta(\varepsilon\nu)^{0.25}S_c^{-n} \quad \text{(S3)}$$

where η is a proportionality constant, v is the kinematic viscosity of water, n is a coefficient representing surface conditions, and

$$\varepsilon = \varepsilon_u + \varepsilon_w \quad \text{(S4)}$$

is the turbulent kinetic energy dissipation rate representing the total contribution from wind shear (ε_u) and waterside convection (ε_w). The wind shear contribution is given by

$$\varepsilon_u = (\tau_t/\rho_w)/(K\delta_v) \quad \text{(S5)}$$

where τ_t is the tangential shear stress in air, ρ_w is the density of water, K is the von Karman constant, and δ_v is the thickness of the viscous sublayer given by Soloviev *et al*. (2007),

$$\delta_v = c_1 v/(\tau_t/\rho_w)^{0.5} \quad \text{(S6)}$$

where c_1 is a dimensionless constant.

The contribution by waterside convection (ε_w) is given as,

$$\varepsilon_w = -\beta \quad \text{(S7)}$$

where β is buoyancy flux defined as

$$\beta = \frac{ga\,Q_e}{\rho_w c_p} \quad \text{(S8)}$$

where g is the acceleration of gravity, a is the thermal expansion coefficient of water, C_p is the specific heat of water, Q_e is the effective surface heat flux (Imberger, 1985; Jeffery *et al*., 2007). If the lake is gaining heat from the atmosphere ($Q_e > 0$), ε_w is set to zero.

We used the air friction velocity measured at PTS to determine τ_t in Equation S5 and S6, and approximate the surface heat flux Q_e as the residual of the surface energy balance equation,

$$Q_e = R_n - H - \lambda E \quad \text{(S9)}$$

where R_n (net radiation), H (sensible heat flux), and λE (latent heat flux) were measured at

PTS. Other coefficients are given by Read *et al*. (2012) as η= 0.29, n = 0.5, and S_c = 600.

The third model, described by MacIntyre *et al*. (2010) and Heiskanen *et al*. (2014), is also a surface renewal parameterization. It uses different fitting coefficients from Read *et al*. (2012) to calculate the gas transfer coefficient,

$$k_3 = 0.5(\varepsilon\nu)^{0.25} S_c^{-n} \quad \text{(S10)}$$

$$\varepsilon = 0.77\ (-\beta) + 0.3\ (u_w^*)^3/(Kz) \quad \text{(S11)}$$

where β is buoyancy flux defined by Equation S8, z is a mixed layer depth, u_w^* is the velocity scale for wind shear given by

$$u_w^* = u_a^* \sqrt{\frac{\rho_a}{\rho_w}} \quad \text{(S12)}$$

where ρ_a is the density of air, u_a^* is the air friction velocity measured at PTS in the lake, S_c is the Schmidt number for CH_4 at in-situ temperature, n = 0.5, and the mixing layer depth z was set to 0.5 m according to the thermal diffusivity profile calculated with the model of Herb and Stephan (2005) for Lake Taihu.

The fourth model is that of Podgrajsek *et al*. (2015) which also considers the effect of waterside convection. The gas transfer coefficient k_4 is given as

$$k_4 = k_1 + 0.05 \times \exp(1068 \times (\beta z)^{1/3}) \quad \text{(S13)}$$

where $k_1$is determined by Equation S1, β is defined by Equation S8, and z is the mixed layer depth. In this equation, the second term represents the contribution of waterside convection to the gas transfer.

We estimated the percentage of the gas transfer (k_w) driven by waterside convection from the last three models. In the case of the second model, k_w was computed from Equation S3 by setting ε_u to zero. In the third and the fourth model, k_w was computed from Equation S10 and S13 by setting u_w^* and k_l to zero, respectively. The percent of the contribution of waterside convection is

$$k_w\% = (k_w/k)100\% \quad \text{(S14)}$$

where k is the total gas transfer coefficient driven by wind shear and waterside convection.

Figure S7 compares the annual mean diffusion flux from the four models. The annual mean CH_4 diffusion fluxes based on the four different diffusivity formulations were 0.092 (Cole *et al*., 1998), 0.103 (Read *et al*., 2012), 0.080 (Heiskanen *et al*., 2014), and 0.093 mmol m^{-2} d^{-1} (Podgrajsek *et al*., 2015).

Figure S7. Comparison of the whole-lake diffusion CH_4 flux calculated with four different models of the gas transfer coefficient. Error bars are one standard deviation of the12 annual mean values for the 29 lake survey locations (Figure 1).

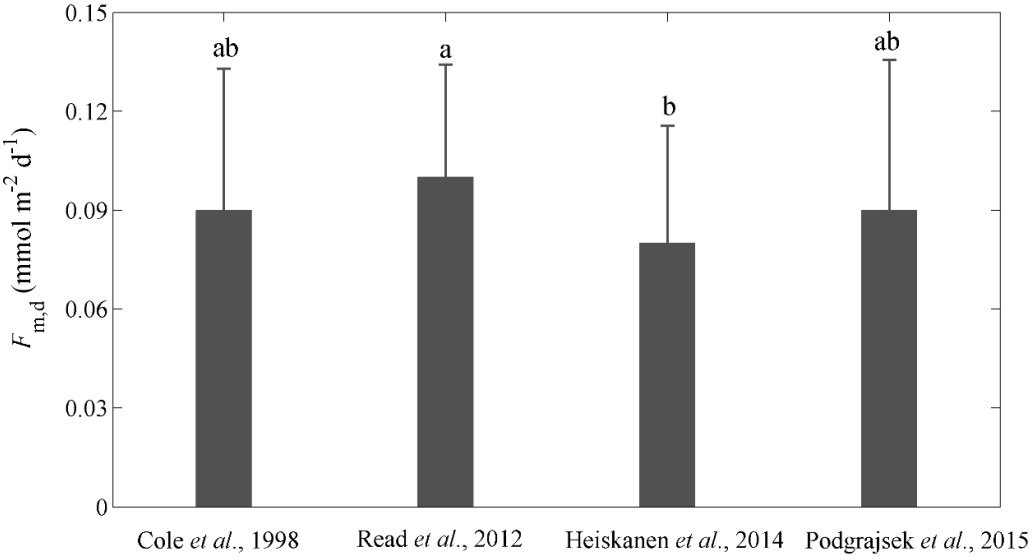

References

Cole, J. J., and N. F. Caraco (1998), Atmospheric exchange of carbon dioxide in a low-wind oligotrophic lake measured by the addition of SF_6, *Limnol. Oceanogr.*, *43*(4), 647-656.

Heiskanen, J., I. Mammarella, S. Haapanala, J. Pumpanen, T. Vesala, S. MacInytre, A. Ojala (2014), Effects of cooling and internal wave motions on gas transfer coefficients in a boreal lake, Tellus B, 66, doi: 10.3402/tellusb.v66.22827.

Herb, W. R., H. G. Stefan (2005), Dynamics of vertical mixing in a shallow lake with submersed macrophytes, Water Resour. Res., 41, W02023, doi:10.1029/2003WR002613

Huotari, J., Ojala, A., Peltomaa, E., et al., (2009), Temporal variation in surface water CO_2 concentration in a boreal humic lake based on high-frequency measurement, Boreal Env. Res. ,14(Suppl. A): 48-60.

Imberger, J. (1985), The diurnal mixed layer, Limnol. Oceanogr., 30(4), 737-770, doi:10.4319/lo.1985.30.4.0737.

Jeffery, C. D., D. K. Woolf, I. S. Robinson, and C. J. Donlon (2007), One-dimensional modeling of convective CO_2 exchange in the tropical Atlantic, Ocean Model., 19(3–4), 161-182, doi:10.1016/j.ocemod.2007.07.003.

Juutinen, S., M. Rantakari, P. Kortelainen, J. T. Huttunen, T. Larmola1, J. Alm, J. Silvola, and P. J. Martikainen, (2009), Methane dynamics in different boreal lake types, Biogeosciences, 6, 209-223.

MacIntyre, S., A. Jonsson, M. Jansson, J. Aberg, D. E. Turney, and S. D. Miller (2010), Buoyancy flux, turbulence, and the gas transfer coefficient in a stratified lake, Geophys. Res. Lett., 37, L24604, doi:10.1029/2010GL044164.

MacIntyre, S., R.Wanninkof, and J. P. Chanton (1995), Trace gas exchange across the air-water interface in freshwater and coastal marine environments, in, edited by: Matson, P. A. and Harriss, R. C., Biogenic trace gases: Measuring emissions from soil and water. Methods in ecology, 52-97, Blackwell Science.

Podgrajsek, E., E. Sahlée, and A. Rutgersson (2015), Diel cycle of lake-air CO_2 flux from a shallow lake and the impact of waterside convection on the transfer velocity, J. Geophys. Res. Biogeosci., 120, 29–38, doi:10.1002/2014JG002781.

Read, J. S., et al. (2012), Lake-size dependency of wind shear and convection as controls on gas exchange, Geophys. Res. Lett., 39(9), doi:10.1029/2012gl051886.

Soloviev, A., M. Donelan, H. Graber, B. Haus, P. Schlüsse (2007), An approach to estimation of near-surface turbulence and CO_2 transfer velocity from remote sensing data, J. Marine Syst., *66*, 182-194.